

1 **Using Eddy Covariance Observations to Determine the Carbon**
2 **Sequestration Characteristics of Subalpine Forests in the Qinghai-**
3 **Tibet Plateau**

4 Niu Zhu^{1,2,4}, Jinniu Wang^{1,2}, Dongliang Luo³, Xufeng Wang³, Cheng Shen^{1,2}, Ning Wu¹
5 1 Chengdu Institute of Biology, Chinese Academy of Sciences, Chengdu 610041,
6 China

7 2 Mangkang Ecological Monitoring Station, Tibet Ecological Security Barrier
8 Ecological Monitoring Network, Qamdo 854500, China

9 3 Northwest Institute of Eco-environmental Resources, Chinese Academy of
10 Sciences, Lanzhou 730000, China

11 4 College of Resources and Environmental Sciences, Gansu Agricultural University,
12 Lanzhou 730070, China

13 **Correspondence:** Jinniu Wang (wangjn@cib.ac.cn)

14 **Abstract:** The subalpine forests are one of the crucial components in the carbon cycling system in
15 the Qinghai-Tibet Plateau (QTP) in the context of climate change and ecosystem dynamics. In this
16 study, we investigated the carbon exchange dynamics for a subalpine forest on the QTP using the
17 eddy covariance method from November 2020 to October 2022. We first revealed the seasonal
18 characteristics of carbon dynamics in the subalpine forest, revealing the pattern of higher rates in
19 summer and autumn and lower rates in winter and spring, and found that autumn is the peak period
20 for carbon sequestration in the subalpine forest. Subsequently, we explored the climatic factors
21 influencing the carbon sequestration function. The PCA analysis show that photosynthetically active
22 radiation (PAR) was major climatic factor driving the net ecosystem exchange (NEE), significantly
23 influencing forest and carbon absorption. The spatial distribution of NEE was significantly
24 positively correlated with temperature, while the average annual precipitation shows a minor effect
25 on NEE at the regional scale. At the annual scale, the subalpine forest was a strong carbon sink, with
26 an average NEE of -342 g C m^{-2} (from November 2020 to October 2022). Despite the challenges
27 caused by climate change, forests remain a robust carbon sink, currently, they are the ecosystems
28 with the highest carbon sequestration capacity in the QTP, with an average annual CO_2 absorption
29 rate of 368 g C m^{-2} . this study provides essential insights for understanding the carbon cycling
30 mechanism in plateau ecosystems and the global carbon balance. We propose that, to positively
31 influence global carbon cycling and promote "carbon neutrality and peak carbon," strengthening the
32 protection and management of subalpine forests is crucial. Although our research has shown that
33 these forest is currently playing a role in continuous carbon absorption, there are significant data
34 gaps on the Qinghai-Tibetan Plateau. Therefore, it is essential to enhance continuous monitoring of
35 forest carbon absorption processes in the future.

36 **Keywords:** Subalpine forest; Qinghai-Tibet Plateau; The eddy covariance system; Three Parallel
37 Rivers Region; Carbon sinks

38 **1 Introduction**

39 Carbon dioxide (CO_2) is a prominent greenhouse gas, and its atmospheric concentration has
40 reached an unprecedented high level in recent years, in May 2021, a recorded peak of 419 parts per
41 million (ppm) was observed at the Mauna Loa Observatory in Hawaii (Stein, 2021). The global
42 atmospheric CO_2 concentration is rapidly increasing at a rate of 2 to 3 ppm per year, compared to

43 pre-industrial levels, the average global temperature has already risen by 1.1 °C by 2019 (World
44 Meteorological Organization, 2019). Human activities have been the primary catalyst behind the
45 significant surge in atmospheric CO₂ concentrations (Schweizer et al., 2020). CO₂ and CH₄
46 collectively contribute approximately 70% to the global warming potential among the six
47 greenhouse gases specified in the Kyoto Protocol (Zhang et al., 2022). As atmospheric CO₂
48 concentrations continue to rise, global climate warming is gradually intensifying. Therefore, The
49 Paris Agreement urges national governments to restrict the increase in global average temperature
50 to well below 2.0 °C above pre-industrial levels and to strive to limit it to 1.5 °C. The increasing
51 atmospheric CO₂ levels will lead to irreversible ecological disasters. For instance, the concentration
52 of CO₂ in the atmosphere is projected to double within approximately 50 years if global
53 consumption of fossil fuels continues to rise at the current rate. Addressing the greenhouse effect
54 caused by carbon dioxide and reducing its impact is a crucial challenge facing human society today.
55 Reducing regional carbon emissions or per capita carbon emissions is widely regarded as an
56 effective approach to carbon reduction (Wang et al., 2023a). Nevertheless, countries around the
57 world have already begun to commit to carbon reduction and carbon neutrality efforts. On
58 September 22, 2020, during the 75th session of the United Nations General Assembly, the Chinese
59 government announced "double carbon" goals, which aim to achieve carbon emission peaking by
60 2030 and carbon neutrality by 2060, in alignment with ecological conservation and sustainable
61 development objectives (Yu, 2022). It is predicted that China's average forest carbon sequestration
62 rate will reach 0.358 Pg C year⁻¹ (petagrams of carbon per year) by 2060 (Cai et al., 2022). This
63 significant rate of carbon sequestration is expected to have a substantial impact on the environment
64 and economy, providing negative feedback to global warming (Pan et al., 2011).

65 Currently, there are various methods available to accurately quantify the carbon sequestration
66 potential of forests, each with its advantages and disadvantages. Quantitative estimation of carbon
67 sequestration potential still requires scientists to establish more *in-situ* sites and generate
68 comprehensive datasets to assess a wide range of areas. Initially, individuals' biomass measurements
69 were used to estimate forest carbon sequestration capacity (Ebermayer, 1876). However, this
70 method was time-consuming, labor-intensive, and prone to inaccuracies due to the omission of
71 various variables during the calculation process. The development of modeling techniques allowed

72 for the use of simulation methods - forest management models and land ecosystem-climate
73 interaction models, such as the Ecological Assimilation of Land and Climate Observation (EALCO),
74 have been widely applied in this regard (Landsberg and Waring, 1997; Wang et al., 2001). Currently,
75 remote sensing monitoring and the eddy covariance method are widely used. Remote sensing
76 techniques can be used to extract vegetation parameters (such as NDVI) from multispectral bands
77 and estimate the carbon sequestration of entire forests through regression analysis (Laurin et al.,
78 2014). The eddy covariance (EC) method, allowing continuous, long-term carbon flux calculation,
79 provides fundamental data for model establishment and calibration. It is widely applied across
80 ecosystems, including urban areas, farmlands, grasslands, forests, and water bodies (Konopka et al.,
81 2021; Vote et al., 2015; Du et al., 2022a; Kondo et al., 2017; Li et al., 2022).

82 The forest ecosystem's Net ecosystem exchange (NEE) of carbon dioxide is influenced by
83 multiple environmental factors. Previous studies have shown that NEE is significantly influenced
84 by air temperature (AT), photosynthetically active radiation (PAR), vapor pressure deficit (VPD),
85 relative humidity (RH), and soil temperature (ST) (Liu et al., 2022). For instance, temperature
86 variables, especially annual or seasonal average temperature variations, serve as the optimal single
87 predictor for carbon flux, explaining variations in carbon flux between 19% and 71% (Banbury
88 Morgan et al., 2021). Photosynthetically active radiation not only influences the absorption of
89 carbon dioxide by the forest canopy but also affects the utilization of carbohydrates by roots due to
90 its association with canopy processes and soil respiration (Baumgartner et al., 2020). Furthermore,
91 research suggests that the NEE is influenced by biotic factors such as NDVI (Normalized Difference
92 Vegetation Index) and LAI (Leaf Area Index) (Tang et al., 2022). Given the projected future global
93 warming trends, the role of forests as a vast carbon reservoir becomes highly significant and worthy
94 of attention. The Qinghai-Tibet Plateau (QTP) is the highest and largest plateau in the world, with
95 an extensive area of alpine forests covering approximately 2.3×10^5 km². These forests hold
96 tremendous economic and ecological benefits. The southeastern region of the QTP boasts one of the
97 world's highest-altitude alpine forest ecosystems. Research indicates that the alpine forest ecosystem
98 in this area has a remarkable capacity to consume methane, reaching up to 5.06 kg ha⁻¹ yr⁻¹, and
99 playing a significant role in mitigating the impact of greenhouse gases (Qu et al., 2023). Since the
100 1960s, the QTP has experienced a faster warming rate than lowland areas. It is projected that this

101 phenomenon will be intensified by the end of the 21st century (Li et al., 2019). Currently, the QTP
102 is considered a weak carbon sink at the overall level, but the carbon source-sink dynamics vary
103 among different ecosystems (Chen et al., 2022). For instance, most lakes in the QTP are currently
104 characterized by supersaturated CO₂ levels (Cole et al., 1994). Mu et al. (2023) found that the
105 thermokarst lakes serve as significant carbon sources through carbon flux measurements in 163
106 thermokarst lakes during the summer and autumn seasons. Wang et al. (2021) discovered that these
107 ecosystems act as sinks for carbon dioxide by comparing carbon fluxes in ten high-mountain
108 ecosystems with different grassland types. The alpine meadows in the eastern QTP were identified
109 as strong carbon sinks, with the highest annual average NEE recorded at -284 g C m⁻². Forest
110 ecosystems play a crucial role in the south-eastern edge of the QTP, providing important support
111 for climate regulation and forestry-based economic activities. Moreover, recent predictive studies
112 suggest that under both current and future climate scenarios, the forested area in this region is
113 expected to expand further, with coniferous forests continuing to grow into higher altitudes (Liu et
114 al., 2021). Due to the extensive presence of permafrost in the QTP, forest net primary productivity
115 exhibits a most pronounced response to surface temperatures in the continuous permafrost zone over
116 multiple years. Therefore, the changes in permafrost in the QTP should not be overlooked, as they
117 also have a significant impact on carbon absorption by forests (Mao et al., 2015). However, the QTP
118 is a vast region with a widespread distribution of high-altitude and subalpine forests. Researchers
119 need to conduct long-term monitoring to understand how these forests will respond to climate
120 change. Furthermore, there is a significant data gap concerning the monitoring of carbon exchange
121 capacity in the forests of the QTP, indicating the need for further data collection efforts. Based on
122 this, we have established a carbon flux monitoring site in the subalpine ecosystem of the Three
123 Parallel Rivers Region, which is located on the south-eastern edge of the QTP and lies in the
124 transitional zone between the QTP and the Yunnan-Kweichow Plateau and is renowned as a global
125 hotspot for biodiversity (Wang et al., 2022). Our research objectives are as follows:

- 126 1) Determine whether the subalpine forests in the Three Parallel Rivers Region act as a carbon
127 sink or source, and quantify the annual uptake or release of carbon dioxide;
- 128 2) Investigate the main environmental factors influencing the carbon exchange process in the
129 subalpine forests and identify the factors with the greatest impact;

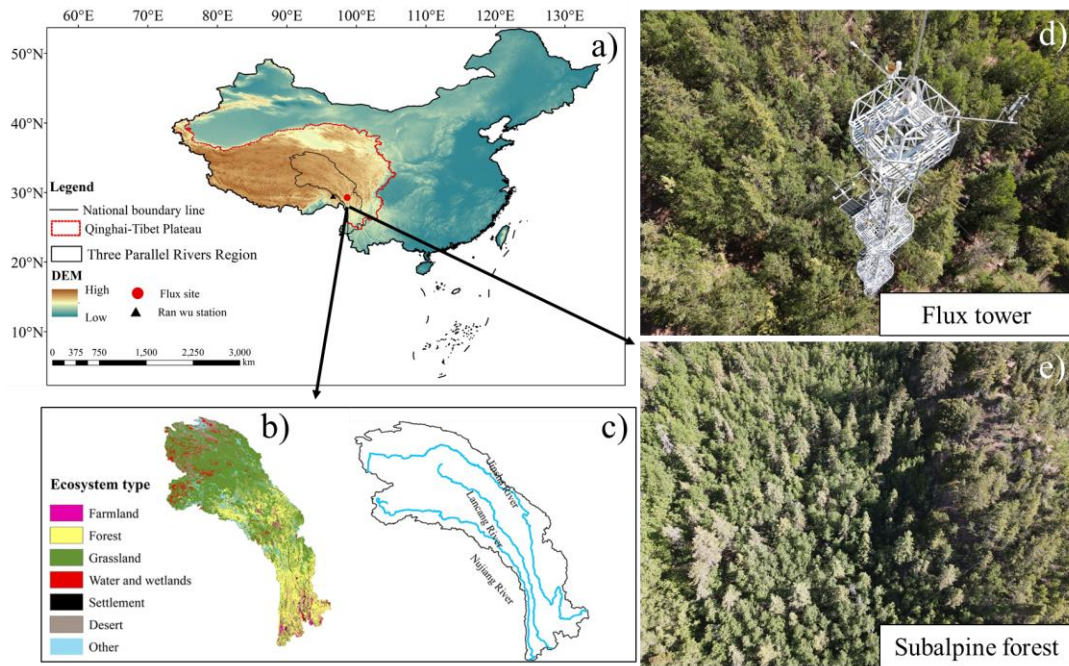
130 3) Since the carbon sink potential of forest ecosystems in the QTP is currently unknown, we
131 evaluated the carbon exchange capacity of subalpine forests by comparing existing data with
132 other ecosystems in the QTP.

133 This study will provide a data foundation and background support for accurately estimating
134 the carbon balance of forests in high-altitude areas and for model simulations in the future.

135 **2 Materials and Methods**

136 2.1 Overview of the study site

137 The study site is located in the Hongla Mountain Yunnan Snub-nosed Monkey National Nature
138 Reserve in Mangkang County, Tibet, China (29.28633 N, 98.69096 E), the core area of the Three
139 Parallel Rivers (Nujiang River, Lancang River, and Jinsha River) Region. The elevation of the study
140 site is 3755 m. The observation period was from November 2020 to October 2022. The study area
141 experiences large diurnal temperature variations and dry conditions in winter, while the summers
142 are warm and humid. The average daily sunshine duration exceeds 10 h, with an annual average
143 temperature of 5 °C and an average annual precipitation of around 600 mm (Niu et al., 2023). The
144 main tree species in the area include *Picea likiangensis* var. *rubescens*, *Abies squamata*, *Sabina*
145 *tibetica* Kom, and *Abies ernestii*. They are accompanied by the growth of some *Quercus*
146 *aquifolioides*, *Rhododendron lapponicum*, and *Potentilla fruticosa* shrubs. The average height of
147 the trees is below 30 meters, and the forest is in a relatively active growth phase, reaching the state
148 of a mature forest. The vegetation coverage ranges from 70% to 80%. The dominant soil type is
149 yellow-brown soil. The mountainous terrain contributes to distinct vertical climate characteristics
150 and significant variations in water and heat conditions. Characterized by numerous dry and hot river
151 valleys and widespread distribution of canyons, the climate in the study area exhibits a clear impact
152 from the southwest and southeast monsoons. The varying elevations give rise to diverse ecosystems,
153 transitioning from alpine forests to mountain shrubs, and above 4000 meters, high alpine grasslands
154 and meadows, forming a noticeable vegetation transition zone. The mountainous topography results
155 in evident vertical climate features and significant fluctuations in water and heat conditions, with
156 precipitation showing a pronouncedly uneven distribution throughout the region (Zemin et al., 2023).



157

158 **Figure 1.** location of the flux site **(a)**. Ecosystem types **(b)** and main rivers **(c)** in Three Parallel
 159 **Rivers Region.** Flux tower **(d)** and forest top view **(e)**. (The national boundary range in the figure
 160 **was retrieved from the <http://bzdt.ch.mnr.gov.cn>, elevation data, and ecosystem type from**
 161 **www.gscloud.cn.)**

162 2.2 Eddy covariance system

163 **The flux data in this study were collected from a 35 m-high tower located at the study site.** At
 164 the top of the tower, a 3-D wind velocity (Wind Master, Gill, UK) and an open-path infrared
 165 CO₂/H₂O analyzer (LI-7500DS, Li-Cor, USA) were installed to measure CO₂ flux. **The instruments**
 166 **had a measurement frequency of 10 Hz.** Additionally, micro-meteorological sensors were placed at
 167 different heights on the tower, **including sensors at 35 m for observing air temperature and humidity**
 168 **(HMP155A, Vaisala, Finland), sensors at -5 cm for soil temperature (TEROS11, LI-Cor, USA), and**
 169 **sensors at 35 m for photosynthetically active radiation (LI-190R, LI-Cor, USA), among other**
 170 **environmental variables. All data were recorded at 30-m intervals and stored in a SmartFlux 3 data**
 171 **logger (Li-Cor, USA) for future download.**

172 2.3 Data processing and quality control

173 **When considering only the turbulent transport of matter and energy in the vertical direction,**
 174 **the carbon dioxide flux (F_c) can be represented by the following equation (Yu and Sun, 2006;**
 175 **Monteith et al., 1994):**

176
$$F_C = \overline{W'CO_2'} \quad (1)$$

177 Where W' is the vertical component of 3-D wind speed fluctuations ($m s^{-1}$), and CO_2' represents the
178 fluctuations in measured CO_2 mole concentration. A positive F_C indicates carbon emissions, while
179 a negative value represents carbon uptake.

180 The acquired 10 Hz raw data was processed and corrected using the EddyPro software
181 (EddyPro 7.06, Li-Cor, USA). The calibration process involved outlier detection for flux data, lag
182 elimination, coordinate rotation (Jia et al., 2020), ultrasonic temperature correction (Schotanus et
183 al., 1983), frequency correction (Moncrieff et al., 1997), and Webb-Pearman-Leuning (WPL)
184 correction (Leuning and King, 1992), After these controls, the integrity of the effective FC raw valid
185 data we obtained reached 92.95 %. We removed outliers caused by environmental disturbances such
186 as power outages, rain, snow, and dust particles that interfered with the instrument. Due to the slope
187 of the underlying surface being around 5 degrees, we also corrected from non-uniform and non-flat
188 surfaces using EddyPro for double coordinate rotation (Cao et al., 2019). As a result, we obtained
189 half-hourly flux data with associated data quality indicators. To evaluate the turbulence steadiness,
190 we employed the "0-1-2" quality assessment method, which classified flux results into three quality
191 levels: 0 for excellent data quality, 1 for moderate data quality, and 2 for low data quality (Mauder
192 and Foken, 2011; Foken et al., 2005). We removed data points labeled with a quality level of "2".
193 We further eliminated flux data with negative values during nighttime since plants do not perform
194 photosynthesis at night. Additionally, we conducted spectral analysis to identify and remove data
195 points with values significantly deviating from normal. Finally, friction velocities (u^*) for each of
196 the two years were determined separately using the method of moving point, and deleted data
197 recorded during nighttime when u^* was less than 0.28 and 0.39 $m s^{-1}$ (Reichstein et al., 2005). After
198 excluding outliers from the data, the data integrity is 72.67%. Tovi software (Tovi, Li-Cor, USA)
199 was used in the process.

200 When turbulence is weak, a portion of CO_2 is stored in the vegetation canopy and the
201 atmosphere below the measurement height. At this time, the NEE is calculated as (Zhang et al.,
202 2018):

203
$$NEE = F_C + F_S \quad (2)$$

204 Where NEE represents the net ecosystem exchange of CO₂, F_C stands for the observed flux during
205 a specific period, F_S represents the CO₂ storage in the forest canopy, F_S is calculated as (Δc/Δt)·h,
206 where Δc is the difference in CO₂ concentration between two consecutive measurements, Δt is the
207 time interval between two consecutive measurements, and h is 35m.

208 We adopted the following formula as a gap-filling strategy for daytime NEE (NEE_{day})
209 concerning PAR, aiming to address missing values during the daytime (Falge et al., 2001):

$$210 \quad NEE_{\text{day}} = \frac{\alpha \cdot \text{PAR} \cdot P_{\text{max}}}{\alpha \cdot \text{PAR} + P_{\text{max}}} - R_{\text{day}} \quad (3)$$

211 where: α (μmol CO₂/μmol PAR) represents the apparent photosynthetic quantum efficiency, which
212 characterizes the maximum efficiency of converting light energy during photosynthesis. PAR (μmol
213 m⁻² s⁻¹) is the photosynthetically active radiation, a measure of the amount of light energy available
214 for photosynthesis. P_{max} (μmol CO₂ m⁻² s⁻¹) is the apparent maximum photosynthetic rate,
215 representing the maximum CO₂ uptake rate under optimal conditions. R_{day} (μmol CO₂ m⁻² s⁻¹) is the
216 daytime dark respiration rate, which denotes the rate of CO₂ release during daylight hours. The
217 parameters α, P_{max}, and R_{day} are obtained through the non-linear fitting of the Michaelis-Menten
218 model to the observed data.

219 During the nighttime, the NEE is modeled using an exponential function of ecosystem
220 respiration and soil temperature to fill in the missing values of NEE during the night (NEE_{night})
221 (Lloyd and Taylor, 1994; Kato et al., 2006):

$$222 \quad NEE_{\text{night}} = a \cdot \exp^{(bt)} \quad (4)$$

223 The parameters *a* and *b* are estimated values for the exponential function used in modeling NEE_{night}.
224 The variable *t* represents the soil temperature measured at the depth of 5 cm. Origin 2023 (Originlab
225 Corporation, USA) is the data processing software used for this analysis. For the missing data,
226 interpolation was performed using Tovi software allows for data interpolation to fill in the gaps and
227 ensure a continuous dataset for further analysis (Reichstein et al., 2005). 27.33% of missing data
228 were interpolated, The final flux data achieved a data integrity of 100%.

229 In flux analysis, the significance of source area contributions cannot be overlooked. In this
230 study, the peak distances of the 90% flux contribution areas averaged over two years are 364.2 and
231 357.1m, respectively. Looking at seasons, the average peak distances of the 90% flux contribution

232 areas for winter, spring, summer, and autumn over the two years are 353.9, 358.2, 350.05, and
233 344.34m, respectively.

234 2.4 Flux partitioning

235 Ecosystem respiration (RE) is the sum of plant and heterotrophic respiration in an ecosystem
236 and is obtained by adding the measured nighttime data to the extrapolated daytime data. Gross
237 primary productivity (GPP) is the total amount of organic carbon fixed by green plants through
238 photosynthesis per unit of time and per unit of area:

$$239 \quad RE = R_{\text{day}} + R_{\text{night}} \quad (5)$$

$$240 \quad GPP = -NEE + RE \quad (6)$$

241 Carbon use efficiency (CUE) is a crucial parameter that reflects the ability of an ecosystem to
242 sequester carbon. It is defined as the ratio of net ecosystem productivity (NEP) to gross primary
243 productivity. CUE can be expressed using the following equation:

$$244 \quad CUE = \frac{NEP}{GPP} = \frac{-NEE}{GPP} \quad (7)$$

245 To study the variation of ecosystem respiration rates with environmental factors, we considered
246 the dependence of nocturnal ecosystem respiration on soil temperature (Pavelka et al., 2007;
247 Mamkin et al., 2023):

$$248 \quad Q_{10} = \exp(10 \cdot \alpha) \quad (8)$$

$$249 \quad \ln(NEE_{\text{night}}) = \alpha \cdot T + \gamma \quad (9)$$

250 Where T is the soil temperature (°C) and γ is an empirical parameter of the equation.

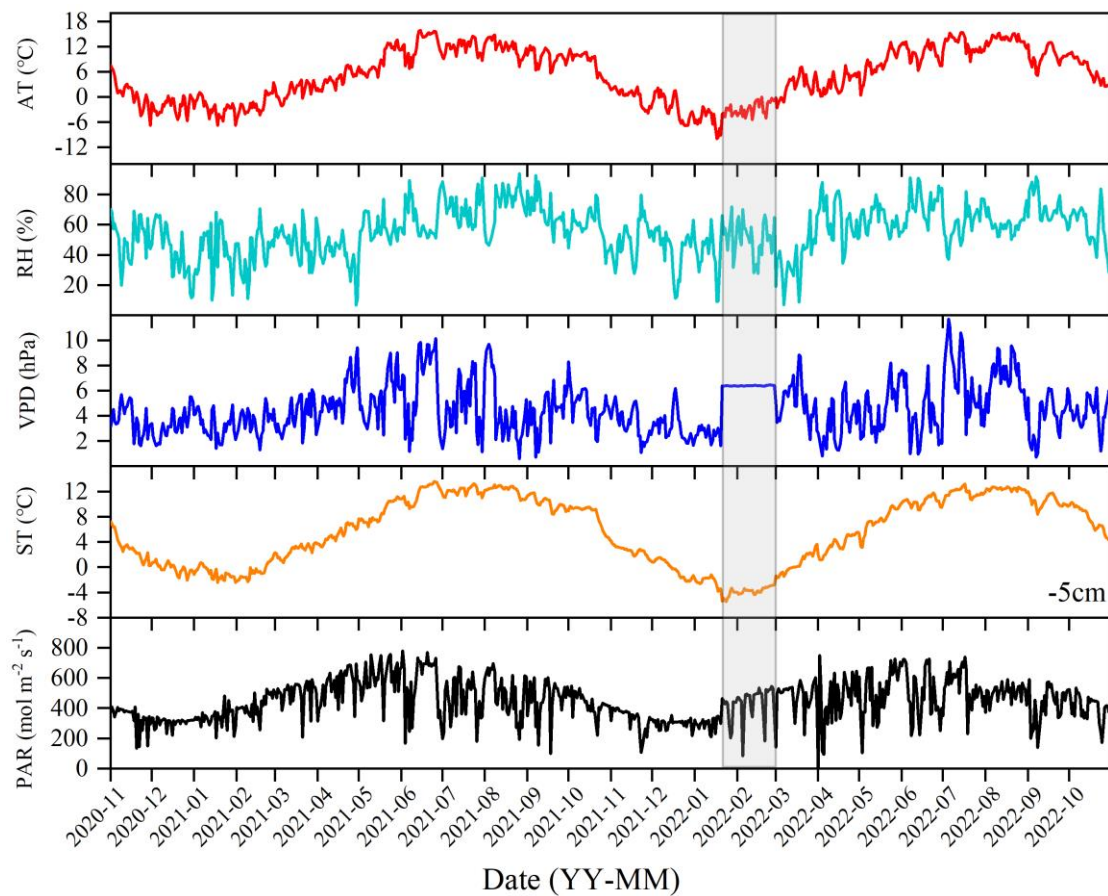
251 To clarify the carbon sink potential of forests in the QTP and to compare it with other
252 ecosystems, a search was conducted in two authoritative databases, Web of Science and China
253 National Knowledge Internet, for research articles on the current utilization of EC systems in the
254 QTP. A total of 82 research results were collected from 48 studies, and their annual average
255 environmental factors, such as air temperature, precipitation, and altitude, were obtained.

256 3 Results

257 3.1 Daily average changes in main environmental factors

258 During the observational period, the environmental conditions exhibited significant
259 fluctuations. The winter and spring seasons were characterized by cold and dry conditions, while
260 the summer and autumn seasons were warm and humid. The daily maximum air temperature (AT)

261 recorded was 15.87 °C (on June 15, 2021), and the minimum temperature was -9.88 °C (on January
 262 17, 2022), with an average of 5.5 °C over the two years. The relative humidity (RH) with an annual
 263 average of 55.89%. The vapor pressure deficit (VPD) with an annual average of 4.46 hPa. Soil
 264 temperature (ST) exhibited a similar trend to air temperature. The highest observed soil temperature
 265 was 13.53 °C (on June 27, 2021), while the minimum was -3.78 °C (on January 18, 2022), with an
 266 annual average of 6.11 °C. Photosynthetically active radiation (PAR) with an annual average of
 267 447.24 mol m⁻² s⁻¹.

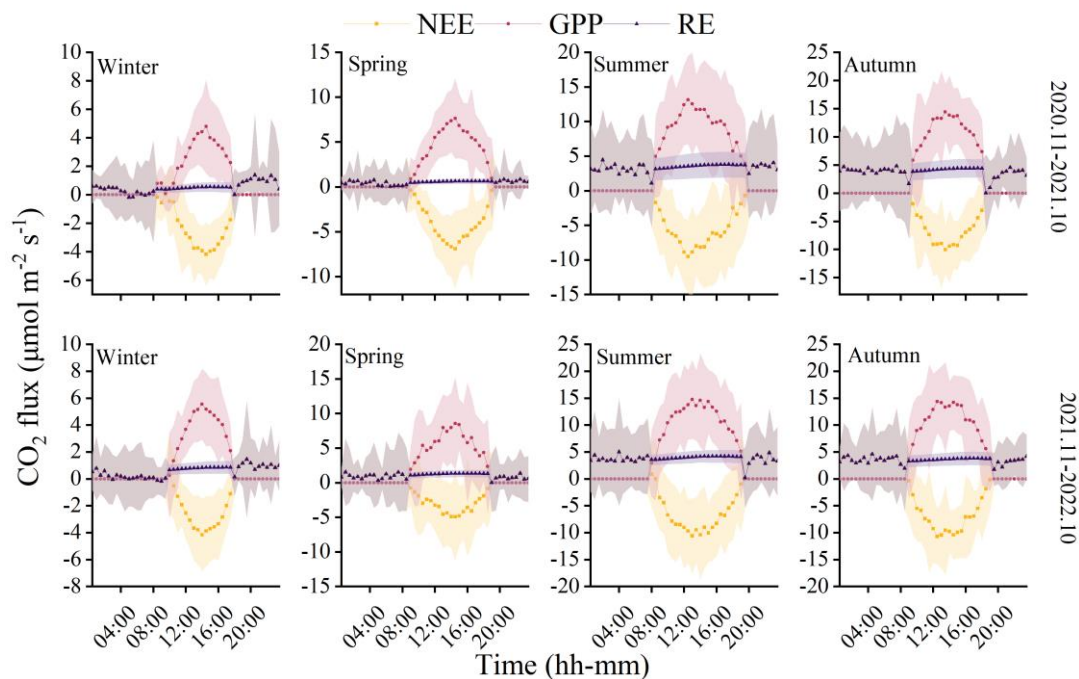


268
 269 Figure 2. Daily values of main environmental factors, air temperature (AT), relative humidity (RH),
 270 vapor pressure deficit (VPD), soil temperature (ST), and Photosynthetically active radiation (PAR).
 271 (The data of the shadow part in the figure comes from the Ranwu forest site (Figure 1). Since there
 272 was no interpolated data source for VPD, the annual average was used instead.)

273 3.2 The seasonal variations in NEE, RE, and GPP

274 The observations from the forest ecosystem indicate distinct diurnal and seasonal variations in
 275 NEE and GPP. The NEE and GPP exhibit a pronounced U-shaped curve, with significant seasonal
 276 differences. The summer and autumn are characterized by peak carbon uptake, with the maximum

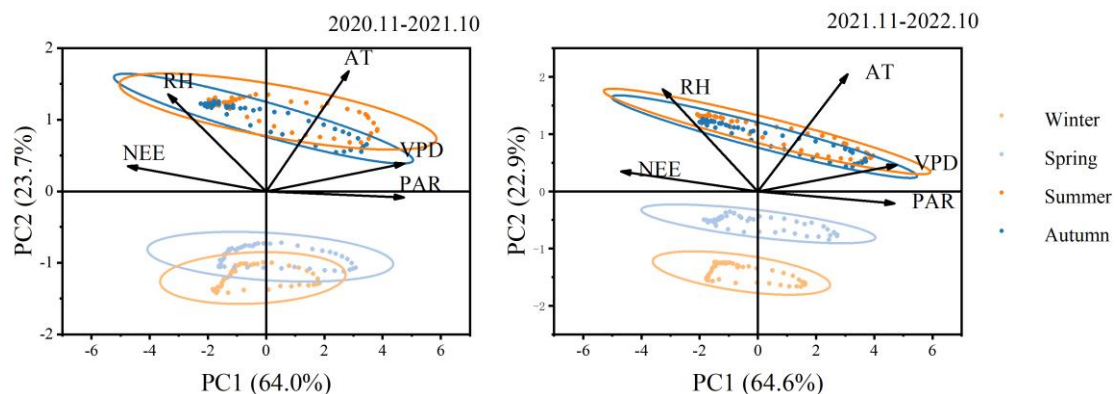
277 **NEE reaching.** During the nighttime, the ecosystem generally releases carbon, while during
 278 favorable daytime meteorological conditions, it demonstrates a carbon uptake capacity. The peak
 279 carbon absorption of the forest ecosystem occurs from 12:00 to 15:00 (**Beijing time, UTC+8:00**).
 280 The **daily carbon sequestration** in summer and autumn is 1.5-3 hrs longer than in winter. The timing
 281 of maximum carbon sequestration capacity changes with each season. **In winter, the transition from**
 282 **nighttime carbon release to daytime carbon uptake occurs around 08:30, which is approximately 1**
 283 **hour later than in summer. GPP characterizes the forest's carbon sequestration capacity, and since**
 284 **photosynthesis does not occur at night, GPP is zero during nighttime. The maximum daily total**
 285 **productivity is recorded at $14.76 \pm 7.34 \mu\text{mol CO}_2 \text{ m}^{-2} \text{ s}^{-1}$ during the summer of the second year,**
 286 **with a standard deviation indicating greater variability in GPP and NEE during the summer and**
 287 **autumn compared to the winter and spring. Although diurnal variations in RE are relatively small,**
 288 **there are significant seasonal differences. During the night, when only respiration occurs, RE equals**
 289 **NEE. However, as photosynthesis becomes active during the day, RE gradually increases and**
 290 **stabilizes. The respiratory rate of the coniferous forest is highest in autumn, being eight times greater**
 291 **than in winter.**



292 **Figure 3. Monthly mean values of carbon fluxes**

293 **3.3 Relationship between NEE and main environmental factors**

295 The PCA analysis of two years of NEE and environmental factors (Figure 4) indicates that the
 296 explanations for the first principal component (PC1) and the second principal component (PC2) are
 297 essentially the same between the two years. The total contributions of PC1 and PC2 are 87.7% and
 298 87.5%, respectively, with PC1 accounting for 64.0% and 64.6% individually. The angle between
 299 photosynthetically active radiation (PAR) and PC1 is minimal, suggesting a strong correlation
 300 between PAR and PC1. Additionally, PAR and VPD contribute the most to PC1, while AT and RH
 301 contribute the most to PC2. The analysis results reveal a significant positive correlation between
 302 NEE and RH, while a significant negative correlation is observed with AT, VPD, and PAR. This
 303 implies that an increase in RH is unfavorable for the forest's absorption of carbon dioxide. Among
 304 these environmental factors, PAR plays a dominant role. Furthermore, the figure illustrates the
 305 relationships between environmental factors, showing a positive correlation between RH and TA,
 306 and a negative correlation with VPD and APR. The indicators exhibit some seasonality, with notable
 307 differences between the winter-spring and summer-autumn seasons, indicating limited similarity
 308 between seasons.

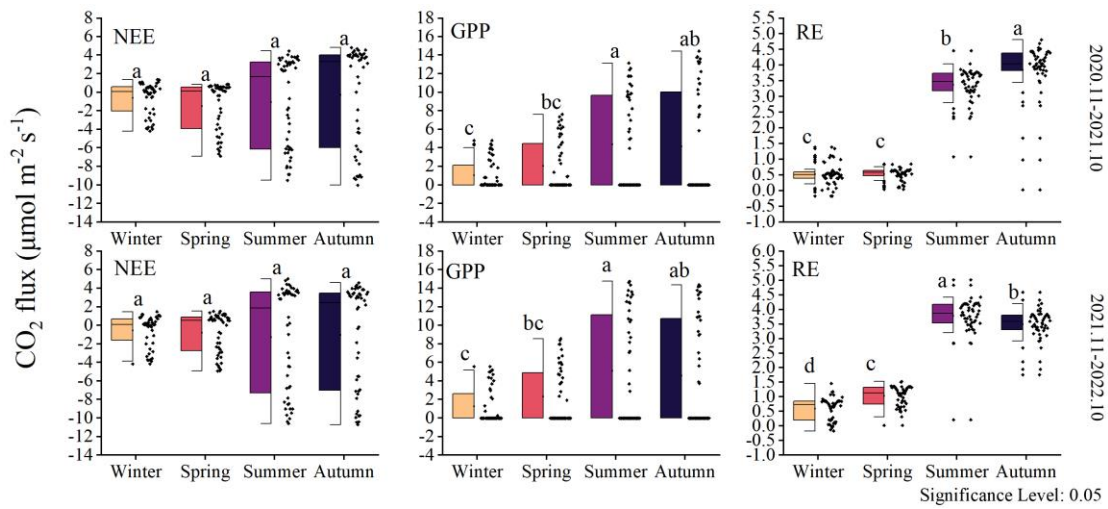


309
310 **Figure 4. Principal component analysis of environmental factors and NEE**

311 3.4 Seasonal variation characteristics of NEE, GPP, and RE

312 The NEE did not show significant inter-seasonal differences (Figure 5). However, data
 313 distribution indicates that the variability in NEE rate differs across different seasons, particularly
 314 between summer-autumn and winter-spring. The changes in GPP over the two years were similar,
 315 with significant differences observed between summer and winter ($P < 0.05$). The RE was higher
 316 during summer-autumn compared to winter-spring. The highest ecosystem respiration occurred in
 317 the first year during autumn, while in the second year, it was highest during summer. Within the
 318 same year, summer and autumn exhibited significant differences ($P < 0.05$), while between the same

319 seasons in different years, notable distinctions were not observed. This pattern is also reflected in
 320 GPP and NEE.



321

322

Figure 5. Seasonal variation of carbon fluxes

323

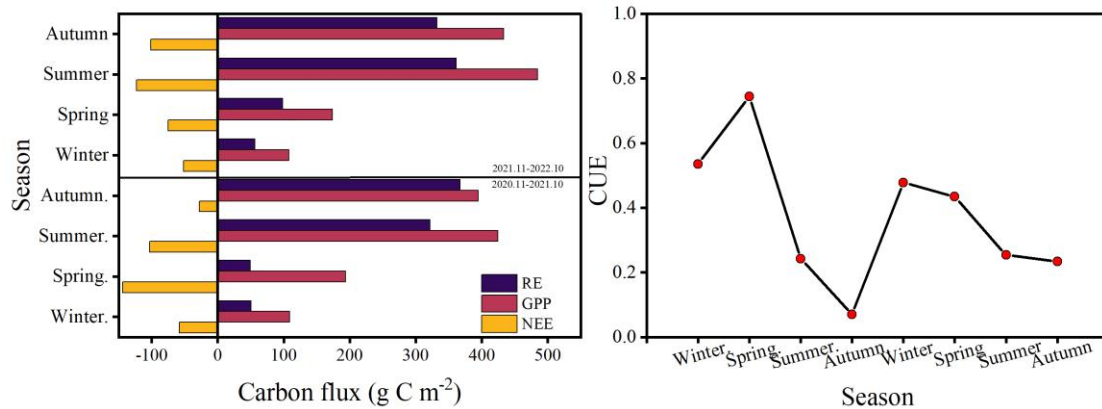
3.5 Changes in total NEE, GPP, RE, and CUE

324

The cumulative fluxes over the two years for the forest ecosystem are shown in Figure 6. NEE indicates the net carbon sequestration in each month. The cumulative respiration reached its highest value of 361 g C m⁻² in the summer of 2022. The total NEE, GPP, and RE for the first year were -332, 1121, and 788 g C m⁻², respectively, and -351, 1199, and 847 g C m⁻² for the second year, respectively. The CUE was higher during the spring and lower during the autumn, with a maximum value of 0.74 and a minimum value of 0.07. The average CUE over the two years was 0.40 and 0.35, respectively.

329

330



331

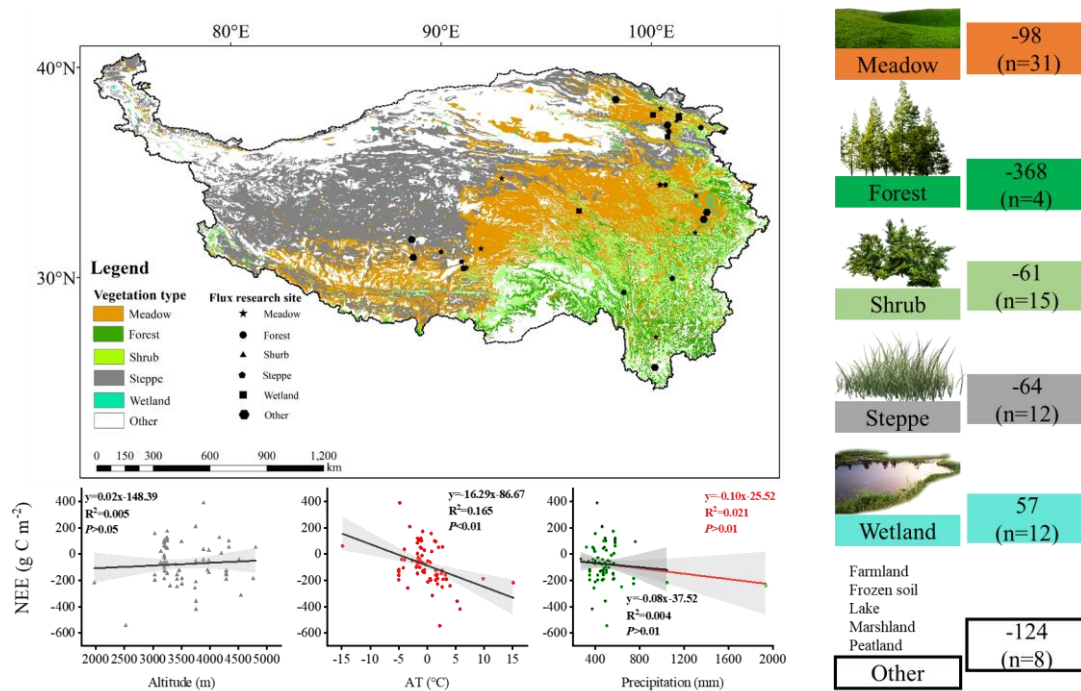
332

Figure 6. Change in total carbon flux and carbon use efficiency

333

3.6 The carbon sequestration potential of subalpine forests of QTP

334 To clarify the carbon sequestration contribution of the subalpine forests found in the QTP, we
 335 compared these research results (Figure 7). Found that ecosystems with high vegetation cover
 336 exhibited higher annual cumulative carbon sequestration. Among these ecosystems, the subalpine
 337 forests in the QTP showed the highest carbon sequestration potential, reaching an average of 368 g
 338 C m⁻² per year. The carbon sequestration potential of different ecosystems ranked as follows: forest >
 339 meadow > steppe > shrub. The average value for wetlands indicated that they are a significant source
 340 of CO₂, releasing 57 g C m⁻² into the atmosphere annually. We also analyzed the influence of altitude,
 341 mean annual air temperature, and precipitation on NEE at these sites in the QTP. It has been
 342 observed that these sites cover a wide range of altitudes, ranging from 1977 to 4800 m. According
 343 to existing results, an increase in elevation may lead to a reduction in carbon uptake, while the range
 344 of mean annual temperature varies between -14.8 to 15.1 °C, and higher mean annual temperatures
 345 significantly increase carbon uptake. Forests exhibit the highest mean annual precipitation,
 346 averaging 827 mm, with mean annual precipitation having a relatively weak impact on the NEE.
 347 These findings highlight the important role of subalpine forests in carbon sequestration in the QTP
 348 and provide insights into the factors that affect carbon exchange in the QTP, such as altitude,
 349 temperature, and precipitation.



350
 351 **Figure 7.** Carbon exchange potential of different ecosystems in the Qinghai-Tibet Plateau

352 **4 Discussion**

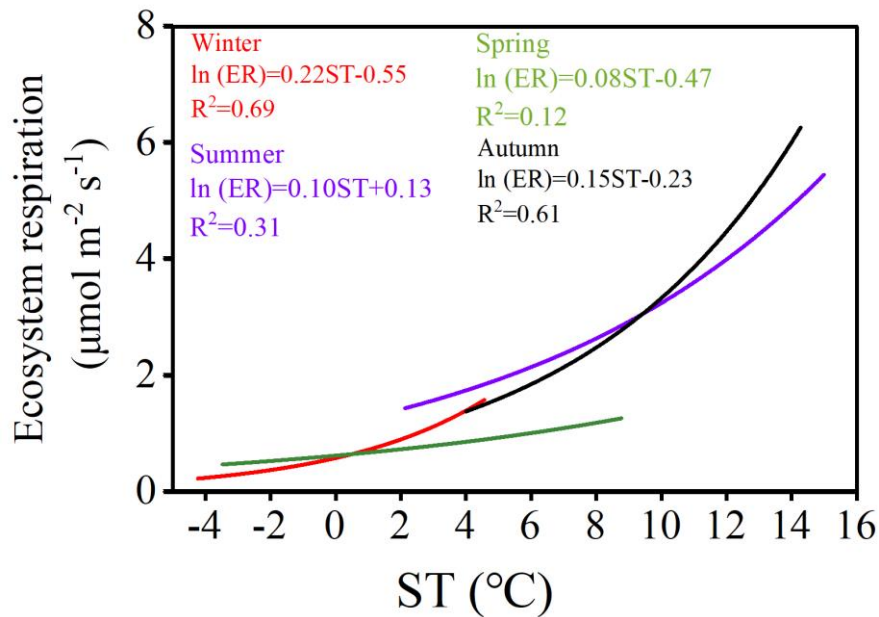
353 4.1 Main factors affecting the carbon sequestration function of subalpine forests

354 Climate change significantly affects the vegetation's carbon sequestration capacity, particularly
355 at the seasonal scale due to phenological changes (Acosta-Hernández et al., 2020). In the short term,
356 these factors (PAR, AT, RH, and VPD) play important roles in regulating vegetation photosynthesis
357 and, consequently, carbon uptake. For instance, PAR representing the portion of solar energy that
358 can be utilized by plants and is an essential component in chloroplast reactions. PAR drives a
359 nonlinear response of GPP to Solar-induced fluorescence (SIF) across different seasons, resulting
360 in a strong positive correlation between GPP and SIF (Wang et al., 2023b). VPD affects
361 photosynthesis and transpiration of leaves, with stomata serving as tiny pores mediating carbon
362 dioxide uptake. Research has demonstrated that excessive increases in VPD are detrimental to
363 photosynthesis. For instance, a moderate increase in VPD significantly reduces photosynthetic
364 efficiency under light fluctuations, due to changes in RH and/or AT often accompany fluctuations
365 in light, studies also indicate that the impact of VPD on sunlight utilization efficiency is primarily
366 determined by relative RH rather than AT (Liu et al., 2024). In different seasons, the same
367 influencing factors exhibit varying degrees of contribution to NEE. For example, during winter,
368 when the climatic conditions are relatively harsh with low air temperature and humidity, the forest
369 maintains a low level of carbon uptake. On longer time scales, such as annual and decadal variations,
370 the inherent changes in forest NEE may be attributed to disturbances and recovery (Hayek et al.,
371 2018). In this study, significant differences in ecosystem respiration were observed during the
372 summer and autumn in different years. Past research suggested that due to leaf aging or water stress,
373 the photosynthetic light use efficiency of the ecosystem peaks after spring leaf expansion and
374 gradually declines (Wehr et al., 2016). This implies a peak in carbon exchange during the summer,
375 followed by higher productivity and ecosystem respiration in the following seasons. The variation
376 in different years may be attributed to rainfall regulating the availability of natural resources such
377 as water, biomass, litter, and soil nutrients (Schwinning and Sala, 2004). For instance, in temperate
378 forests, when microbial biomass undergoes seasonal changes, microbial activity exhibits a seasonal
379 lag in response to temperature variation, resulting in a seasonally delayed effect between litter
380 heterotrophic respiration and temperature (Ataka et al., 2020). Whether such differences persist
381 between different years on longer time scales remains to be demonstrated through more sustained

382 and detailed research in the future. Ecosystem respiration sensitivity to temperature is represented
383 by the Q_{10} coefficient. In this study, seasonal variations influenced the magnitude of Q_{10} (as shown
384 in Figure 8). The calculated Q_{10} for each season are as follows: 9.025, 2.22, 2.71, and 4.48. The
385 winter season exhibited the highest sensitivity of forest ecosystem respiration to temperature,
386 indicating that respiration rates in the winter are more responsive to changes in temperature
387 compared to other seasons. The main reason for such differences is that ecosystem respiration
388 consists of heterotrophic respiration and autotrophic respiration, which are typically governed by
389 different factors (Edwards, 1975). For instance, the high activity of soil microbes contributes to
390 heterotrophic respiration, a process dominated by soil temperature and moisture conditions, which
391 are severely restricted during the cold and dry conditions of winter (Falge et al., 2002).
392 Simultaneously, due to the changing relative roles of growth and maintenance respiration, the
393 allocation of autotrophic respiration varies seasonally. In winter, soil CO_2 emissions constitute a
394 significant portion of ecosystem CO_2 emissions, and in some boreal forests, the ratio between the
395 two can reach 0.6 or even higher (Davidson et al., 2006). In winter, under the frequent coverage of
396 snow, cold-adapted microorganisms thriving in a relatively narrow sub-zero temperature range
397 engage in respiration and exhibit relatively high sensitivity to warming or cooling beyond this range
398 (Monson et al., 2006). The seasonal patterns of the Q_{10} value are jointly determined by the variation
399 in the ratio of soil respiration to ecosystem respiration, reflecting these seasonal changes.

400 Our integrated analysis (as shown in Figure 7) reveals that despite the high elevation of the
401 "Third Pole", the topographic factor of elevation does not have a significant impact on carbon uptake.
402 Instead, NEE gradually increases with a steep rise in elevation. Research conducted by Wang et al.
403 (2023c) indicates that mean annual average temperature and precipitation are the main driving
404 factors of interannual variations in NEE in alpine meadows and alpine steppes. Decreased
405 precipitation resulting in a transition into carbon sources at some regions with high precipitation-
406 dependent alpine grasslands. It is worth noting that, among all data collection sites, alpine wetlands
407 show an average carbon source trend. Due to prolonged flooding and low temperatures, microbial
408 activity in alpine wetlands is hindered, and the accumulation of organic carbon from plant litter
409 decomposition is substantial. As a result, approximately 57 g C m^{-2} is emitted into the atmosphere

410 annually. Previous studies have indicated that NEE in alpine wetlands is increasing with global
411 warming (Yasin et al., 2022).



412

413 **Figure 8.** Relationship between NEE_{night} and soil temperature in different seasons

414 4.2 Sustained carbon sequestration of subalpine forests

415 Subalpine forests are integral components of global alpine ecosystems and play crucial roles
416 in the global carbon cycle. Our study on subalpine forests demonstrates a continuous absorbing of
417 carbon dioxide even during winter, which aligns well with measurements taken in the vicinity of
418 Mount Fuji in Japan (Mizoguchi et al., 2012). The age of subalpine forests is a crucial factor
419 influencing sustained carbon sequestration. Based on NPP simulations of natural subalpine forests
420 in the Northern Rockies, Carey. (2001) found that aboveground net primary productivity reaches its
421 maximum after approximately 250 years, followed by a decline, this challenges the previous view
422 that forests older than 100 years are generally considered to be unimportant carbon sinks. **Compared**
423 **to the forest (mature forest) of Mount Gongga in the QTP (e.g., Zhang et al., 2018), the subalpine**
424 **forest in this study exhibits a stronger carbon sequestration capacity.** However, its carbon
425 sequestration ability is slightly weaker than that of the Qilian Mountains high-mountain forests
426 (approximately 60-70 years old) in the QTP (Zhang et al., 2018; Du et al., 2022b). Although existing
427 flux monitoring results of high-altitude forests in the QTP indicate that these forest ecosystems act
428 as carbon sinks, it is important to consider that globally there are still many cold regions with
429 coniferous forests serve as carbon sources. For example, continuous CO₂ flux monitoring from

430 native boreal forests in Sweden for over 10 years indicates that they are a net carbon source, which
431 is attributed to the contribution of woody debris to RE due to disturbances such as extreme weather
432 events, fires, insect infestations, and pathogen attacks (Hadden and Grelle, 2017). In the summer of
433 2018, Europe experienced a heatwave that affected the carbon cycling in forests. The mixed
434 coniferous-deciduous forest in southern Estonian, under the influence of the heatwave, transitioned
435 from a net carbon sink to a net carbon source in 2018 (Krasnova et al., 2022). Particular attention
436 should be paid to the long-term monitoring in high-altitude environments of the impact of
437 disturbances on forest carbon sequestration capacity. Our study has shown that forests in the QTP
438 have the strongest carbon sink capacity, indicating that alpine forests will have an important
439 sustained effect on carbon reduction in the QTP in the context of future climate change, but whether
440 this sustained effect will be longer than other ecosystems is still unknown. However, a modeling
441 experiment in a large semi-arid area of California predicted that grasslands are more resilient carbon
442 sinks than forests in responding to climate change in the 21st century (Dass et al., 2018). In terms
443 of carbon sequestration rate, forests in the QTP were significantly stronger than other ecosystems,
444 followed by grasslands, while alpine deserts and alpine grasslands in the north-western and southern
445 regions were the main carbon sources (Wu et al., 2022). Forests are mostly distributed in the south-
446 eastern margin of the QTP and the mid-altitude area near 3000 m in the Sichuan-Tibet alpine gorge
447 area, with an area of $19.3 \times 10^4 \text{ km}^2$ (Yu et al., 2022). Based on the average value of a few current
448 carbon flux monitoring, the forest in the QTP will absorb about $71 \times 10^6 \text{ Mg C year}^{-1}$.

449 **5 Conclusion**

450 This study explores the carbon sequestration function, seasonal variations, and climate drivers
451 of subalpine forests in the QTP. Over the observational period, We synchronously monitored
452 ecosystem carbon exchange and primary environmental factors using an eddy covariance system.
453 The research reveals that the subalpine forest is a carbon sink, with a total NEE, GPP, and RE of -
454 332, 1121, and 788 g C m^{-2} , respectively, and -351, 1199, and 847 g C m^{-2} for two years, respectively.
455 Photosynthetically active radiation was identified as the primary control of NEE. The NEE did not
456 exhibit significant differences across seasons. Combining results from other eddy covariance sites
457 on the QTP, this study highlights those forests have the highest carbon sequestration potential,
458 reaching 368 g C m^{-2} annually, followed by meadows, steppes, and shrubs. Wetlands, however,

459 were identified as a substantial carbon dioxide source. Despite the challenges posed by climate
460 change, the subalpine forests in the QTP retain substantial carbon sequestration potential.
461 Strengthening conservation and management efforts for subalpine forests is crucial to ensure their
462 continued and significant carbon sequestration function in the future. Overall, this research
463 underscores the vital role of subalpine forests in the QTP as essential carbon sink regions, playing
464 a critical role in the context of global climate change.

465 **Data availability.** The data is available from the authors on request.

466 **Authorship contributions.** **Niu Zhu:** Conceptualization, study design, data analyses,
467 visualization, writing-original draft. **JinNiu Wang:** study design, writing—review & editing,
468 supervision, project administration, funding acquisition. **Dongliang Luo and Xufeng Wang:**
469 writing-reviewing & editing. **Cheng Shen and Ning Wu:** resources, data curation, supervision. all
470 authors approved the final manuscript.

471 **Declaration of competing interest.** The authors declare that they have no conflict of interest.

472 **Acknowledgements.** We thank Ms. Neha Bisht for her substantial comments and language
473 revision to improve the manuscript. This study was funded by CAS "Light of West China" Program
474 (2021XBZG-XBQNXZ-A-007); The National Natural Science Foundation of China (31971436);
475 The State Key Laboratory of Cryospheric Science, Northwest Institute of Eco-Environment and
476 Resources, Chinese Academy Sciences (SKLCS-OP-2021-06).

477 **Reference**

478 Acosta-Hernández, A. C., Padilla-Martínez, J. R., Hernández-Díaz, J. C., Prieto-Ruiz, J. A., Goche-Telles,
479 J. R., Nájera-Luna, J. A., and Pompa-García, M.: Influence of Climate on Carbon Sequestration in
480 Conifers Growing under Contrasting Hydro-Climatic Conditions, *Forests*, 11, 1134, 2020.

481 Ataka, M., Kominami, Y., Sato, K., and Yoshimura, K.: Microbial Biomass Drives Seasonal Hysteresis
482 in Litter Heterotrophic Respiration in Relation to Temperature in a Warm-Temperate Forest, *Journal of*
483 *Geophysical Research: Biogeosciences*, 125, e2020JG005729, <https://doi.org/10.1029/2020JG005729>,
484 2020.

485 Banbury Morgan, R., Herrmann, V., Kunert, N., Bond-Lamberty, B., Muller-Landau, H. C., and
486 Anderson-Teixeira, K. J.: Global patterns of forest autotrophic carbon fluxes, *Global Change Biology*,
487 27, 2840-2855, <https://doi.org/10.1111/gcb.15574>, 2021.

488 Baumgartner, S., Barthel, M., Drake, T. W., Bauters, M., Makelele, I. A., Mugula, J. K., Summerauer, L.,
489 Gallarotti, N., Cizungu Ntaboba, L., Van Oost, K., Boeckx, P., Doetterl, S., Werner, R. A., and Six, J.:
490 Seasonality, drivers, and isotopic composition of soil CO₂ fluxes from tropical forests of the Congo Basin,
491 *Biogeosciences*, 17, 6207-6218, 10.5194/bg-17-6207-2020, 2020.

492 Cai, W., He, N., Li, M., Xu, L., Wang, L., Zhu, J., Zeng, N., Yan, P., Si, G., and Zhang, X.: Carbon
493 sequestration of Chinese forests from 2010 to 2060: Spatiotemporal dynamics and its regulatory
494 strategies, *Science Bulletin*, 67, 836-843, 2022.

495 Cao, S., Cao, G., Chen, K., Han, G., Liu, Y., Yang, Y., and Li, X.: Characteristics of CO₂, water vapor,
496 and energy exchanges at a headwater wetland ecosystem of the Qinghai Lake, *Canadian Journal of Soil
497 Science*, 99, 227-243, 10.1139/cjss-2018-0104, 2019.

498 Carey, E. V., Sala, A., Keane, R., and Callaway, R. M.: Are old forests underestimated as global carbon
499 sinks?, *Global Change Biology*, 7, 339-344, 10.1046/j.1365-2486.2001.00418.x, 2001.

500 Chen, H., Ju, P. J., Zhu, Q., Xu, X. L., Wu, N., Gao, Y. H., Feng, X. J., Tian, J. Q., Niu, S. L., Zhang, Y.
501 J., Peng, C. H., and Wang, Y. F.: Carbon and nitrogen cycling on the Qinghai-Tibetan Plateau, *NATURE
502 REVIEWS EARTH & ENVIRONMENT*, 3, 701-716, 10.1038/s43017-022-00344-2, 2022.

503 Cole, J. J., Caraco, N. F., Kling, G. W., and Kratz, T. K.: Carbon dioxide supersaturation in the surface
504 waters of lakes, *Science*, 265, 1568-1570, 1994.

505 Dass, P., Houlton, B. Z., Wang, Y., and Warlind, D.: Grasslands may be more reliable carbon sinks than
506 forests in California, *Environmental Research Letters*, 13, 074027, 10.1088/1748-9326/aacb39, 2018.

507 Davidson, E. A., Richardson, A. D., Savage, K. E., and Hollinger, D. Y.: A distinct seasonal pattern of
508 the ratio of soil respiration to total ecosystem respiration in a spruce-dominated forest, *Global Change
509 Biology*, 12, 230-239, <https://doi.org/10.1111/j.1365-2486.2005.01062.x>, 2006.

510 Du, C., Zhou, G., and Gao, Y.: Grazing exclusion alters carbon flux of alpine meadow in the Tibetan
511 Plateau, *Agricultural and Forest Meteorology*, 314, 108774, 2022a.

512 Du, Y., Pei, W., Zhou, H., Li, J., Wang, Y., and Chen, K.: Net ecosystem exchange of carbon dioxide
513 fluxes and its driving mechanism in the forests on the Tibetan Plateau, *Biochemical Systematics and
514 Ecology*, 103, 10.1016/j.bse.2022.104451, 2022b.

515 Ebermayer, E.: Die gesammte Lehre der Waldstreu mit Rücksicht auf die chemische Statik des
516 Waldbaues: unter Zugrundlegung der in den Königl. Staatsforsten Bayerns angestellten Untersuchungen,

517 Springer1876.

518 Edwards, N. T.: Effects of Temperature and Moisture on Carbon Dioxide Evolution in a Mixed Deciduous
519 Forest Floor, *Soil Science Society of America Journal*, 39, 361-365,
520 <https://doi.org/10.2136/sssaj1975.03615995003900020034x>, 1975.

521 Falge, E., Baldocchi, D., Tenhunen, J., Aubinet, M., Bakwin, P., Berbigier, P., Bernhofer, C., Burba, G.,
522 Clement, R., Davis, K. J., Elbers, J. A., Goldstein, A. H., Grelle, A., Granier, A., Guðmundsson, J.,
523 Hollinger, D., Kowalski, A. S., Katul, G., Law, B. E., Malhi, Y., Meyers, T., Monson, R. K., Munger, J.
524 W., Oechel, W., Paw U, K. T., Pilegaard, K., Rannik, Ü., Rebmann, C., Suyker, A., Valentini, R., Wilson,
525 K., and Wofsy, S.: Seasonality of ecosystem respiration and gross primary production as derived from
526 FLUXNET measurements, *Agricultural and Forest Meteorology*, 113, 53-74,
527 [https://doi.org/10.1016/S0168-1923\(02\)00102-8](https://doi.org/10.1016/S0168-1923(02)00102-8), 2002.

528 Falge, E., Baldocchi, D., Olson, R., Anthoni, P., Aubinet, M., Bernhofer, C., Burba, G., Ceulemans, R.,
529 Clement, R., Dolman, H., Granier, A., Gross, P., Grünwald, T., Hollinger, D., Jensen, N.-O., Katul, G.,
530 Keronen, P., Kowalski, A., Lai, C. T., Law, B. E., Meyers, T., Moncrieff, J., Moors, E., Munger, J. W.,
531 Pilegaard, K., Rannik, Ü., Rebmann, C., Suyker, A., Tenhunen, J., Tu, K., Verma, S., Vesala, T., Wilson,
532 K., and Wofsy, S.: Gap filling strategies for defensible annual sums of net ecosystem exchange,
533 *Agricultural and Forest Meteorology*, 107, 43-69, [https://doi.org/10.1016/S0168-1923\(00\)00225-2](https://doi.org/10.1016/S0168-1923(00)00225-2), 2001.

534 Foken, T., Göckede, M., Mauder, M., Mahrt, L., Amiro, B., and Munger, W.: Post-Field Data Quality
535 Control, in: *Handbook of Micrometeorology: A Guide for Surface Flux Measurement and Analysis*,
536 edited by: Lee, X., Massman, W., and Law, B., Springer Netherlands, Dordrecht, 181-208, 10.1007/1-
537 4020-2265-4_9, 2005.

538 Hadden, D. and Grelle, A.: Net CO₂ emissions from a primary boreo-nemoral forest over a 10year period,
539 *Forest Ecology and Management*, 398, 164-173, <https://doi.org/10.1016/j.foreco.2017.05.008>, 2017.

540 Hayek, M. N., Longo, M., Wu, J., Smith, M. N., Restrepo-Coupe, N., Tapajos, R., da Silva, R., Fitzjarrald,
541 D. R., Camargo, P. B., Hutryra, L. R., Alves, L. F., Daube, B., Munger, J. W., Wiedemann, K. T., Saleska,
542 S. R., and Wofsy, S. C.: Carbon exchange in an Amazon forest: from hours to years, *Biogeosciences*, 15,
543 4833-4848, 10.5194/bg-15-4833-2018, 2018.

544 Jia, X., Mu, Y., Zha, T., Wang, B., Qin, S., and Tian, Y.: Seasonal and interannual variations in ecosystem
545 respiration in relation to temperature, moisture, and productivity in a temperate semi-arid shrubland,

546 Science of The Total Environment, 709, 136210, <https://doi.org/10.1016/j.scitotenv.2019.136210>, 2020.

547 KATO, T., TANG, Y., GU, S., HIROTA, M., DU, M., LI, Y., and ZHAO, X.: Temperature and biomass
548 influences on interannual changes in CO₂ exchange in an alpine meadow on the Qinghai-Tibetan Plateau,
549 Global Change Biology, 12, 1285-1298, <https://doi.org/10.1111/j.1365-2486.2006.01153.x>, 2006.

550 Kondo, M., Saitoh, T. M., Sato, H., and Ichii, K.: Comprehensive synthesis of spatial variability in carbon
551 flux across monsoon Asian forests, Agricultural and Forest Meteorology, 232, 623-634, 2017.

552 Konopka, J., Heusinger, J., and Weber, S.: Extensive Urban Green Roof Shows Consistent Annual Net
553 Uptake of Carbon as Documented by 5 Years of Eddy-Covariance Flux Measurements, Journal of
554 Geophysical Research: Biogeosciences, 126, e2020JG005879, 2021.

555 Krasnova, A., Mander, Ü., Noe, S. M., Uri, V., Krasnov, D., and Soosaar, K.: Hemiboreal forests' CO₂
556 fluxes response to the European 2018 heatwave, Agricultural and Forest Meteorology, 323, 109042,
557 <https://doi.org/10.1016/j.agrformet.2022.109042>, 2022.

558 Landsberg, J. and Waring, R.: A generalised model of forest productivity using simplified concepts of
559 radiation-use efficiency, carbon balance and partitioning, Forest ecology and management, 95, 209-228,
560 1997.

561 Laurin, G. V., Chen, Q., Lindsell, J. A., Coomes, D. A., Del Frate, F., Guerriero, L., Pirotti, F., and
562 Valentini, R.: Above ground biomass estimation in an African tropical forest with lidar and hyperspectral
563 data, ISPRS Journal of Photogrammetry and Remote Sensing, 89, 49-58, 2014.

564 Leuning, R. and King, K. M.: Comparison of eddy-covariance measurements of CO₂ fluxes by open-
565 and closed-path CO₂ analysers, Boundary-Layer Meteorology, 59, 297-311, 10.1007/BF00119818, 1992.

566 Li, L., Zhang, Y., Wu, J., Li, S., Zhang, B., Zu, J., Zhang, H., Ding, M., and Paudel, B.: Increasing
567 sensitivity of alpine grasslands to climate variability along an elevational gradient on the Qinghai-Tibet
568 Plateau, Science of the Total Environment, 678, 21-29, 2019.

569 Li, X. Y., Shi, F. Z., Ma, Y. J., Zhao, S. J., and Wei, J. Q.: Significant winter CO₂ uptake by saline lakes
570 on the Qinghai-Tibet Plateau, Global Change Biology, 28, 2041-2052, 2022.

571 Liu, C., Wu, Z., Hu, Z., Yin, N., Islam, A. T., and Wei, Z.: Characteristics and influencing factors of
572 carbon fluxes in winter wheat fields under elevated CO₂ concentration, Environmental Pollution, 307,
573 119480, 2022.

574 Liu, J., Zou, H.-X., Bachelot, B., Dong, T., Zhu, Z., Liao, Y., Plenković-Moraj, A., and Wu, Y.: Predicting

575 the responses of subalpine forest landscape dynamics to climate change on the eastern Tibetan Plateau,
576 *Global Change Biology*, 27, 4352-4366, <https://doi.org/10.1111/gcb.15727>, 2021.

577 Liu, N.-Y., Yang, Q.-Y., Wang, J.-H., Zhang, S.-B., Yang, Y.-J., and Huang, W.: Differential Effects of
578 Increasing Vapor Pressure Deficit on Photosynthesis at Steady State and Fluctuating Light, *Journal of*
579 *Plant Growth Regulation*, 10.1007/s00344-024-11268-0, 2024.

580 Lloyd, J. and Taylor, J. A.: On the temperature dependence of soil respiration, *Functional Ecology*, 8,
581 315-323, 1994.

582 Mamkin, V., Avilov, V., Ivanov, D., Varlagin, A., and Kurbatova, J.: Interannual variability in the
583 ecosystem CO₂ fluxes at a paludified spruce forest and ombrotrophic bog in the southern taiga,
584 *Atmospheric Chemistry and Physics*, 23, 2273-2291, 10.5194/acp-23-2273-2023, 2023.

585 Mao, D., Luo, L., Wang, Z., Zhang, C., and Ren, C.: Variations in net primary productivity and its
586 relationships with warming climate in the permafrost zone of the Tibetan Plateau, *Journal of*
587 *Geographical Sciences*, 25, 967-977, 10.1007/s11442-015-1213-8, 2015.

588 Mauder, M. and Foken, T.: Documentation and Instruction Manual of the Eddy-Covariance Software
589 Package TK3 (update),

590 Mizoguchi, Y., Ohtani, Y., Takanashi, S., Iwata, H., Yasuda, Y., and Nakai, Y.: Seasonal and interannual
591 variation in net ecosystem production of an evergreen needleleaf forest in Japan, *Journal of Forest*
592 *Research*, 17, 283-295, 10.1007/s10310-011-0307-0, 2012.

593 Moncrieff, J. B., Massheder, J. M., de Bruin, H., Elbers, J., Friborg, T., Heusinkveld, B., Kabat, P., Scott,
594 S., Soegaard, H., and Verhoef, A.: A system to measure surface fluxes of momentum, sensible heat, water
595 vapour and carbon dioxide, *Journal of Hydrology*, 188-189, 589-611, <https://doi.org/10.1016/S0022->
596 1694(96)03194-0, 1997.

597 Monson, R. K., Lipson, D. L., Burns, S. P., Turnipseed, A. A., Delany, A. C., Williams, M. W., and
598 Schmidt, S. K.: Winter forest soil respiration controlled by climate and microbial community
599 composition, *Nature*, 439, 711-714, 10.1038/nature04555, 2006.

600 Monteith, J. L., Unsworth, M. H., and Webb, A.: Principles of environmental physics, *Quarterly Journal*
601 *of the Royal Meteorological Society*, 120, 1699, 1994.

602 Mu, C., Mu, M., Wu, X., Jia, L., Fan, C., Peng, X., Ping, C. I., Wu, Q., Xiao, C., and Liu, J.: High carbon
603 emissions from thermokarst lakes and their determinants in the Tibet Plateau, *Global Change Biology*,

604 2023.

605 Niu, Z., Jinniu, W., Xufeng, W., Dongliang, L., Cheng, S., and Aihong, G.: Net ecosystem CO₂ exchange
606 and its influencing factors in non-growing season at a sub-alpine forest in the core Three Parallel Rivers
607 region, *Acta Ecologica Sinica*, 43, 5967-5979, 10.5846/stxb202204020841, 2023.

608 World Meteorological Organization.: 2019 concludes a decade of exceptional global heat and high-
609 impactweather[EB/OL].[https://public.wmo.int/en/media/press-release/2019-concludes-decade-of-](https://public.wmo.int/en/media/press-release/2019-concludes-decade-of-exceptional-global-heat-and-high-impact-weather)
610 [exceptional-global-heat-and-high-impact-weather](https://public.wmo.int/en/media/press-release/2019-concludes-decade-of-exceptional-global-heat-and-high-impact-weather), 2019.

611 Pan, Y., Birdsey, R. A., Fang, J., Houghton, R., Kauppi, P. E., Kurz, W. A., Phillips, O. L., Shvidenko, A.,
612 Lewis, S. L., and Canadell, J. G.: A large and persistent carbon sink in the world's forests, *Science*, 333,
613 988-993, 2011.

614 Pavelka, M., Acosta, M., Marek, M. V., Kutsch, W., and Janous, D.: Dependence of the Q10 values on
615 the depth of the soil temperature measuring point, *Plant and Soil*, 292, 171-179, 10.1007/s11104-007-
616 9213-9, 2007.

617 Qu, S., Xu, R., Yu, J., and Borjigidai, A.: Extensive atmospheric methane consumption by alpine forests
618 on Tibetan Plateau, *Agricultural and Forest Meteorology*, 339, 109589,
619 <https://doi.org/10.1016/j.agrformet.2023.109589>, 2023.

620 Reichstein, M., Falge, E., Baldocchi, D., Papale, D., Aubinet, M., Berbigier, P., Bernhofer, C., Buchmann,
621 N., Gilmanov, T., Granier, A., Grünwald, T., Havránková, K., Ilvesniemi, H., Janous, D., Knohl, A.,
622 Laurila, T., Lohila, A., Loustau, D., Matteucci, G., Meyers, T., Miglietta, F., Ourcival, J.-M., Pumpanen,
623 J., Rambal, S., Rotenberg, E., Sanz, M., Tenhunen, J., Seufert, G., Vaccari, F., Vesala, T., Yakir, D., and
624 Valentini, R.: On the separation of net ecosystem exchange into assimilation and ecosystem respiration:
625 review and improved algorithm, *Global Change Biology*, 11, 1424-1439, [https://doi.org/10.1111/j.1365-](https://doi.org/10.1111/j.1365-2486.2005.001002.x)
626 [2486.2005.001002.x](https://doi.org/10.1111/j.1365-2486.2005.001002.x), 2005.

627 Schotanus, P., Nieuwstadt, F. T. M., and De Bruin, H. A. R.: Temperature measurement with a sonic
628 anemometer and its application to heat and moisture fluxes, *Boundary-Layer Meteorology*, 26, 81-93,
629 10.1007/BF00164332, 1983.

630 Schweizer, V. J., Ebi, K. L., van Vuuren, D. P., Jacoby, H. D., Riahi, K., Strefler, J., Takahashi, K., van
631 Ruijven, B. J., and Weyant, J. P.: Integrated Climate-Change Assessment Scenarios and Carbon Dioxide
632 Removal, *One Earth*, 3, 166-172, 10.1016/j.oneear.2020.08.001, 2020.

633 Schwinning, S. and Sala, O. E.: Hierarchy of responses to resource pulses in arid and semi-arid
634 ecosystems, *Oecologia*, 141, 211-220, 10.1007/s00442-004-1520-8, 2004.

635 Stein, T.: Carbon dioxide peaks near 420 parts per million at Mauna Loa observatory, NOAA Research,
636 June, 7, 2021.

637 Tang, X., Xiao, J., Ma, M., Yang, H., Li, X., Ding, Z., Yu, P., Zhang, Y., Wu, C., Huang, J., and Thompson,
638 J. R.: Satellite evidence for China's leading role in restoring vegetation productivity over global karst
639 ecosystems, *Forest Ecology and Management*, 507, 120000,
640 <https://doi.org/10.1016/j.foreco.2021.120000>, 2022.

641 Vote, C., Hall, A., and Charlton, P.: Carbon dioxide, water and energy fluxes of irrigated broad-acre crops
642 in an Australian semi-arid climate zone, *Environmental Earth Sciences*, 73, 449-465, 2015.

643 Wang, C.-Y., Wang, J.-N., Wang, X.-F., Luo, D.-L., Wei, Y.-Q., Cui, X., Wu, N., and Bagaria, P.:
644 Phenological Changes in Alpine Grasslands and Their Influencing Factors in Seasonally Frozen Ground
645 Regions Across the Three Parallel Rivers Region, Qinghai-Tibet Plateau, *Frontiers in Earth Science*, 9,
646 10.3389/feart.2021.797928, 2022.

647 Wang, S., Grant, R., Versegny, D., and Black, T.: Modelling plant carbon and nitrogen dynamics of a
648 boreal aspen forest in CLASS—the Canadian Land Surface Scheme, *Ecological Modelling*, 142, 135-
649 154, 2001.

650 Wang, Y., Yao, G., Zuo, Y., and Wu, Q.: Implications of global carbon governance for corporate carbon
651 emissions reduction, *Frontiers in Environmental Science*, 11, 3, 2023a.

652 Wang, Y., Sun, Y., Chen, Y., Wu, C., Huang, C., Li, C., and Tang, X.: Non-linear correlations exist
653 between solar-induced chlorophyll fluorescence and canopy photosynthesis in a subtropical evergreen
654 forest in Southwest China, *Ecological Indicators*, 157, 111311,
655 <https://doi.org/10.1016/j.ecolind.2023.111311>, 2023b.

656 Wang, Y., Xiao, J., Ma, Y., Ding, J., Chen, X., Ding, Z., and Luo, Y.: Persistent and enhanced carbon
657 sequestration capacity of alpine grasslands on Earth's Third Pole, *Science Advances*, 9,
658 eade6875, doi:10.1126/sciadv.ade6875, 2023c.

659 Wang, Y., Xiao, J., Ma, Y., Luo, Y., Hu, Z., Li, F., Li, Y., Gu, L., Li, Z., and Yuan, L.: Carbon fluxes and
660 environmental controls across different alpine grassland types on the Tibetan Plateau, *Agricultural and
661 Forest Meteorology*, 311, 108694, 2021.

662 Wehr, R., Munger, J. W., McManus, J. B., Nelson, D. D., Zahniser, M. S., Davidson, E. A., Wofsy, S. C.,
663 and Saleska, S. R.: Seasonality of temperate forest photosynthesis and daytime respiration, *Nature*, 534,
664 680-683, 10.1038/nature17966, 2016.

665 Wu, T., Ma, W., Wu, X., Li, R., Qiao, Y., Li, X., Yue, G., Zhu, X., and Ni, J.: Weakening of carbon sink
666 on the Qinghai–Tibet Plateau, *Geoderma*, 412, 115707, <https://doi.org/10.1016/j.geoderma.2022.115707>,
667 2022.

668 Y, W. Z., Y, L. Z., K, D. S., L, F. M., S, L. Y., M, L. S., N, W. S., H, M. C., X, M. T., and Y, C.: Evolution
669 of ecological patterns and its driving factors on Qinghai-Tibet Plateau over the past 40 years, *Acta*
670 *Ecologica Sinica*, 42, 8941-8952, 2022.

671 Yasin, A., Niu, B., Chen, Z., Hu, Y., Yang, X., Li, Y., Zhang, G., Li, F., and Hou, W.: Effect of warming
672 on the carbon flux of the alpine wetland on the Qinghai-Tibet Plateau, *Frontiers in Earth Science*, 10,
673 10.3389/feart.2022.935641, 2022.

674 YU, G. and SUN, X.: Principles of flux measurement in terrestrial ecosystem, Beijing: Higher Education
675 Press, 2006.

676 Yu, Y.: Double-order system construction of China s climate change legislation under the dual carbon
677 goals, *China Population Resources and Environment*, 32, 89-96, 2022.

678 Zemin, Z., Fenggui, L., Qiong, C., Xingsheng, X., and Qiang, Z.: Spatial Prediction of Potential Property
679 Loss by Geological Hazards based on Random Forest—A Case Study of Chamdo, Tibet, *Plateau Science*
680 *Research*, 7, 21-30, 10.16249/j.cnki.2096-4617.2023.02.003, 2023.

681 Zhang, J., Lin, H., Li, S., Yang, E., Ding, Y., Bai, Y., and Zhou, Y.: Accurate gas extraction (AGE) under
682 the dual-carbon background: Green low-carbon development pathway and prospect, *Journal of Cleaner*
683 *Production*, 134372, 2022.

684 Zhang, Y., Zhu, W., Sun, X., and Hu, Z.: Carbon dioxide flux characteristics in an *Abies fabri* mature
685 forest on Gongga Mountain, Sichuan, China, *Acta Ecologica Sinica*, 38, 6125-6135, 2018.

686